

# Demodulation and Vibration Signal Systems for Photonic Fiber Optic Pressure Sensor

Aliya Kalizhanova<sup>1</sup>, Murat Kunelbayev<sup>2\*</sup>, Waldemar Wojcik<sup>3</sup>, Ainur Kozbakova<sup>2</sup>,  
Baydaulet Urmashiev<sup>2</sup>, Assiyat Akhsutova<sup>4</sup>

<sup>1</sup>Institute of Information and Computational Technologies CS MSHE RK,  
Almaty University of Power Engineering and Telecommunications after G. Daukeyev,  
Almaty 050040, Kazakhstan

<sup>2</sup>Institute of Information and Computer Technologies, Al-Farabi Kazakh National University,  
Almaty 050040, Kazakhstan

<sup>3</sup>Lublin University of Technologies,  
Lublin, 20-618, Poland

<sup>4</sup>Almaty University of Power Engineering and Telecommunications after G. Daukeyev,  
Almaty 050040, Kazakhstan

Received: April 15, 2023. Revised: November 4, 2023. Accepted: December 23, 2023. Published: February 7, 2024.

**Abstract**—The article describes the optical elements of signal demodulation and polling systems from photonic pressure sensors on inclined fiber Bragg gratings, which are often used to measure the refractive index (RI). A new design of a photonic fiber-optic Bragg pressure sensor with an inclined lattice has been developed, which is connected to standard multimode fibers with an inclined Bragg lattice connected to a metal diaphragm, which is a deformed inclined cantilever. The light source is polarized using the first polarizer and directed to the photonic crystal fiber in such a way as to excite multimode fibers. In this work, a method was developed for determining the optical elements of the spectral contour length system, which consists of setting the cut-off wavelength and then determining the accompanying refractive index. An experimental study determined the curve of the chain length change in the set. To process random signals, the spatial correlation method is used in combination with an approach to digital images based on the number of lanes and the direction of movement. The experimental results differ from the theoretical ones by about 4%. The developed correlation method reflects frequency as well as randomness, it is used in the photographic process together with the image correction given in this document.

**Keywords**—Demodulation, vibration, titled Bragg gratings, photonic fiber-optic sensors, pressure sensor with tilted Bragg grating, polarized, deformation

## I. INTRODUCTION

In the work [1], were developed optical fibers as transmitters, which were used in various areas of sensor usage, they have such advantages as small weight and sizes, resistance to environmental exposure, or the possibility of remote sounder.

In the research herein there was developed method of recording on optic fiber of periodic structure and created the Bragg grating.

An important solution of the given method is no necessity to destroy the optic fiber structure by removing its cladding.

Figure 1 shows an FBG in which the periodic modulation scheme is uniformly distributed (or tilted) by an angle of  $h$  relative to the fiber axis, thus, in addition to connecting to the mode of the opposite distribution of the core, the core mode can be effectively connected to circular and non-circular symmetric, jointly distributed or reciprocally distributed coating modes, which depends on from the tilt angle TFBG.

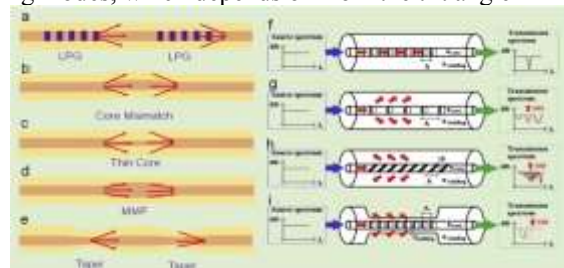


Fig. 1 (a–e) configurations and light transmittance of MZIS different types: a) LPG pair, b) core mismatching, c) SMF with a thin core, d) segment MMF and e) fiber restriction (f–i). Main configurations of fiber gratings: f) standard fiber Bragg grating, g) standard long-period grating; h) tilted fiber Bragg grating; i) etched fiber Bragg grating (SRI: surrounding refractive index). Reprinted by authority of [1].

In tilted fiber Bragg grating the light is connected not only to reciprocally distributed core mode, but also with reciprocally distributed cladding modes. Depending on the changing of the core refractive index tilted angle in the grating transmittance spectrum there appear narrow peaks, each of which conforms to one cladding mode. Main Bragg wavelength depends on the effective refractive index of the core  $n_{core}$  and grating period  $\Lambda$  of the core perturbation RI:

$$\lambda_{FBG} = 2 * n_{core} * \Lambda \quad (1)$$

For FBG grating the peaks of separate cladding modes are located in shorter range of wavelengths, than the main Bragg peak:

$$\lambda_{TFBG} = (n_{core} - n_{clad(m)}) \frac{\Lambda}{\cos(\theta)} \quad (2)$$

where -  $n_{clad(m)}$  effective refractive index of  $m$  coating mode. In standard FBG there exist several dozens of cladding modes, and they create an outstanding dense spectral block terminal of narrow-band resonances.

In the work [2], there was measured the grating spectrum with the big tilted angle of cladding mode, which appears further from the main Bragg peak (for shorter waves).

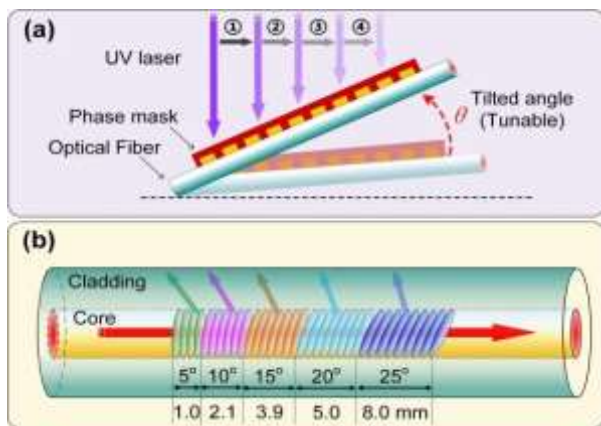


Fig. 2 (a) Technique of signing writing on the tilted grating for assumed multangular FBG and (b) configuration of grating distribution in fiber core, [2].

Figure 2 shows the signature technique on the inclined lattice for the proposed polygonal FBG, as well as the configuration of the lattice distribution in the fiber core. As can be seen from this figure, the refractive index was measured with significantly lower values, at which the greatest angle of inclination also reduces the intensity of the main Bragg mode. In the technique described here, SIR range extensions have been studied that could use a lattice consisting of several gratings with different angles of inclination. The article [3], presents the setup of femtosecond laser recording along the plane.

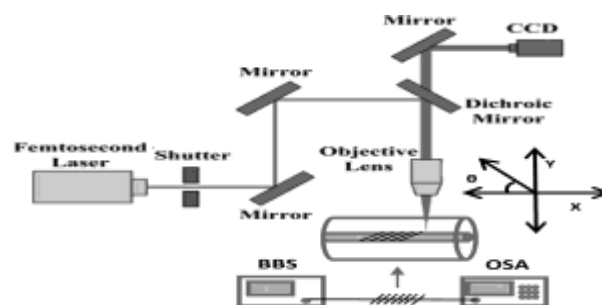


Fig. 3 Set of femtosecond laser writing. CCD, device with charged connection; BBS, wideband light source; OSA, optical spectrum analyzer, [3]

In the article, 3 shows a set for femtosecond laser recording, which was created by the elastic method of direct recording behind the plane for the development of specially created inclined fiber Bragg gratings using a femtosecond laser. The laser inscription is applied using a fiber coating. At the same time, the lattice planes are adjusted in such a way as to minimize birefringence, with precise control of the position of the wavelength and the strength of the coating systems. In these intervals, tenth-order lattices were designed in such a way that higher-order lattices could be studied at shorter wavelengths.

Figure 3 shows the customized label. The FBG spectrum labels were reconstructed using a broadband light source and an optical spectrum analyzer. The fiber samples were mounted on high-precision movement stages with an air bearing, which allows controlled movement during the inscription procedure. The planes deposited by the laser had a width of  $\approx 800$  nm. At the same time, other dimensions were controlled by a suitable displacement of the displacement stage, which led to a three-dimensional change in the refractive index with a controlled plane length, depth, and angle of the lattice plane. The pulse energy at the laser output was measured as 100 J per pulse with a repetition rate of 50 kHz. The modified structures were selectively applied to the fibers in a repeatable manner. The fiber shell was not removed, which allowed the integrity of the fiber to be preserved throughout the initial laser treatment.

Additionally, to SRI measurement, tilted Bragg gratings might be used, also, as a band [4], and rotation sensors [5], [6]. There are many FBG spectrum demodulation techniques. They might be broken down as follows:

- techniques, using the spectrum of all weld deposition modes (global techniques),
- methods, using wavelength displacement in the single cladding mode, [7].



Fig. 4 (on-line color) Photo of packed sensor (mainly, connected piece of the fiber with 25 mm length to FBG along the fiber length out of connection), [7].

Figure 4 shows the packed sensor: actually, a piece of fiber, connected to FBG near the far end, coated with gold. That configuration, as well, secures the sensor operation without deformation to eliminate cross-sensitivity to deformation of cladding modes of higher order.

Techniques, using displacement of the wavelength of the only coating mode, shall be based on the modes, close to the border of clipping, as, in that case, they are more sensitive. The disadvantage of that solution is limited measurement volume with usage of one mode and extreme non-linear dependence of displacement on SRI changes. In [8], an experiment is presented measuring the displacement of Bragg modes and shells can be clearly determined using the ALL method. Thus, simultaneous two-parameter measurement using only one TMF BG sensor is implemented. The work [9], offered to widen the method by means of wavelet transformation. Transformation maintains noise attenuation in the spectrum and definition of modes wavelengths peak displacement on the basis of filtered shift spectrum (wavelet-coefficients).

The first type of techniques (global methods методы), in turn, might be broken down as follows:

- techniques, using cladding modes amplitudes for computing such parameters, as square, occupied by mantle modes, [10], statistical parameters (asymmetry and excess), [11], or standard cladding modes spectrum deviation from its, average value, [12],

- In [13], [14], the means of determining wavelength cutoffs are shown, while individual shell modes are not transmitted and begin to flow out of the shell.

In the work [15], there was developed an aerial method, which in addition to the SRI definition, as well, might be used, applying TFBG grating to specify the liquid level.

The most important herein is the vibration control system. The core of the technique is in measuring the spectrum's own (or induced) oscillations of studied data, analyzing spectra harmonics, and proceeding from which there are drawn conclusions on defects presented in subsystems. Currently, there exists a high-frequency electrical spectrum to conduct the works on creating analogous systems, using fiber-optic sensors. The principal advantages of optical sensors, compared to electrical ones are the electromagnetic field's sensitive element; small sizes and weight; and the simplicity of uniting a lot of sensors into groups.

The work [16], considered the main types of optical vibration sensors. The articles [17], [18], [19], [20], [21], [22], [23], [24], [25], showed the optical sensors operation principle in registering optical signals power change, and a simultaneous displacement of transmitting and receiving fibers. Figure 5, presents one of the noncontact sensor's versions.

Figure 5 shows the flow diagram of non-contact vibration sensor. The sensor's activity brings to the minimum the sensor's own construction influence on measurements. Interferometric sensor has a shortage, based on intensity modulation, it is their low accuracy. Accuracy upgrading might be reached through measurement transformation into the spectral area.

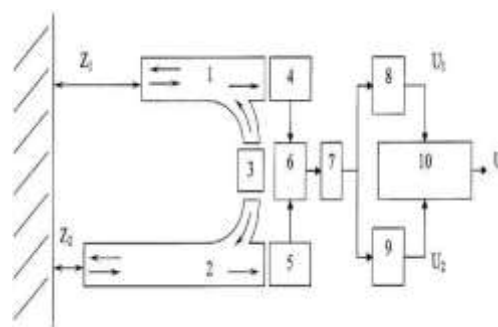


Fig. 5 Flow diagram of noncontact vibration sensor, [18]. 1, 2-optical fibers, 3 – light source, 4, 5 – optical modulators, 6 – photodetector, 7 – amplifier, 8, 9 – filters, 10 – processor; Z1, Z2 – distance between fiber edges and subject to control, U1, U2 – informational signals of two shoulders, U – calculated signal.

For signal processing, there is the most frequently used Fabry-Perot interferometer, consisting of two parallel plane reflective surfaces. Distinction of such sensors from noncontact sensors is in the fact, that information is fed into the signal's spectrum, which permits to raise sufficiently the sensitivity and resolution.

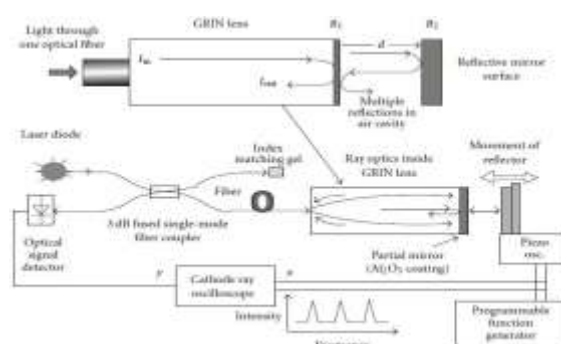


Fig. 6 Vibration sensor on the basis of Fabry-Perot interferometer, [12].

The works [26], [27], [28], have considered optical sensors on the basis of fiber Bragg gratings. Based on FBG, the vibration sensors operation principle is in the transformation of inertia mass's induced oscillations energy into Bragg gratings deformation. The articles [29], [30], presented FBG temperature sensitivity, used in various schemes (Figure 6).

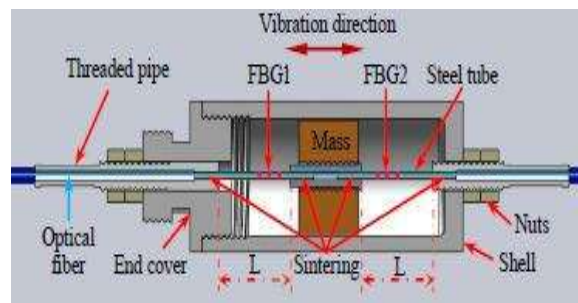


Fig. 7 Differential vibration sensor on FBG basis, [29]

Figure 7 shows a differential vibration sensor on an FBG basis. To register signals in the sensors thereof there used

special devices – interrogation units, representing a spectrometer with a combined radiation source.

The works [31], [32], demonstrate approaches to constructing interrogation systems, where information search frequency is sufficiently higher. The shortage of such an approach is the complexity of sensor multiplexing. In the article, [33], herein there is considered computation of temperature, deformation and pressure in engineering and building structures, using fiber Bragg grating (FBG). There has been studied fiber Bragg sensors in combination with the technology of far infrared range sensors, both for simultaneous temperature and deformation definition and for synchronous definition of temperature and pressure. Developed fiber-optic refractometric sensor for controlling technological and building structures health. Computations showed, that displacement change in percentage, in respect to the wavelength, varies for 5 temperature values from 20 to 100°C, which proves, that displacement changes linearly and proportionally to the wavelength, and it is connected with fiber plasticity, which increases along with temperature raise and boosts humidifying in fiber, consequently, displacement decreases.

The purpose of this study is to experimental work of a demodulation system and vibration signals for a photonic fiber-optic pressure sensor.

## II. MATERIALS AND METHODS

In 2022, experts from the Institute of Information and Computing Technologies of the Ministry of Education and Science of the Republic of Kazakhstan came up with and studied a fiber-optic refractometer. The novelty of the work herein is the development of a photonic fiber-optic pressure sensor with Bragg tilted grating, which presents sufficient simplification of medium refractive index measurement system, as well, it does not require the usage of spectrophotometer, analyzers of optical spectrum and algorithms of optical spectrum analysis. An important feature of the model herein is the special metal diaphragm, which, being deformed rejects the cantilever, whereby, gratings are recorded on the same multimode fiber. In addition, there is photonic-crystal fiber, which induces multimode fibers.

The photonic fiber-optic pressure sensor with tilted Bragg grating is illustrated with drawings in Figure 8.

The fiber-optic sensor was fabricated in compliance with the utility model. Ultraviolet excimer laser 1 ejects beams. There are multimode optical fibers 2 with tilted Bragg grating, which is connected to special metal diaphragm 4 and cantilever 5. Also, there are polarizers 6 and 8, photonic-crystal fiber 7 and photodetector 9.

The offered sensor operates as follows:

Photonic fiber-optic pressure sensor consists of ultraviolet excimer laser 1, connected through a multimode optical fiber to tilted Bragg grating 3, which is coupled with a special metal diaphragm 4, which, being deformed rejects cantilever 5. Cantilever rejection increases the sensitivity to temperature, pressure, and curve.

Afterward, the laser beam is polarized in the first polarizer 6 and sent to photonic-crystal fiber 7 accordingly, inducing multimode fibers.

The second polarizer 8 permits the laser beam from multimode fiber to interfere, and optical response is measured by means of photodetector 9.

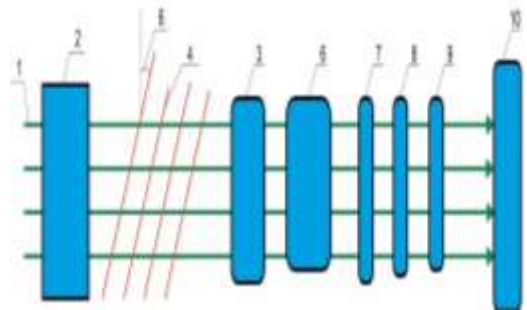


Fig. 8 Photonic fiber-optic pressure sensor with tilted Bragg grating. The difference is that the broadband tilt pressure sensor is connected via a multimode optical fiber to an optical connector, and the output of the first optical connector is connected via a connected multimode optical fiber, to which a photodetector is additionally connected.

## III. RESULTS

Measurements of photonic fiber-optic pressure sensor with tilted Bragg grating emerged into the water with a salt solution.

Used grating had a tilt angle  $\theta = 8$  and was maintained, using the phase mask method. Spectrum measurements were carried out with 0,01 Nm definition.

Researchers did their best to maintain the grating so as to avoid additional curves. Figure 9 shows the transmittance spectrum of the grating, positioned in the air (SRI = 1). The grating spectrum is mainly affected by tilt angle, grating length, refractive index modulation depth and its distribution along the grating length (apodization).

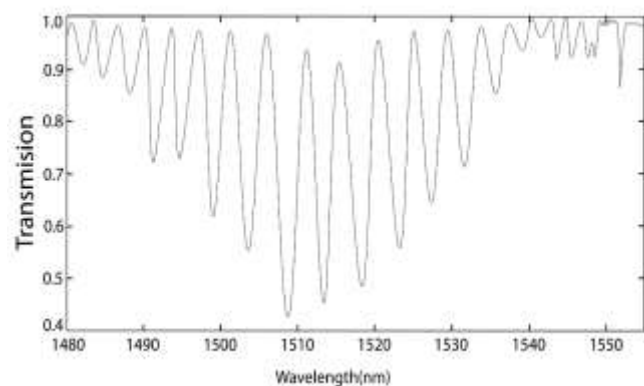


Fig. 9 Spectrum of photonic fiber-optic pressure sensor with tilted Bragg grating, positioned in the air

It is seen from the Figure 9, that the cladding modes disappear in proportion to SRI increase.

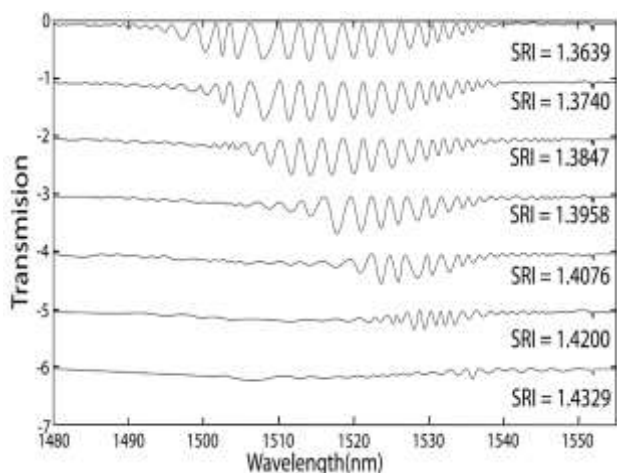


Fig. 10 Spectra of photonic fiber-optic pressure sensor with tilted Bragg grating were placed into water with salt solution for several hours

Figure 10 (in the left) shows interrelation between the normalized circuit length and SRI.

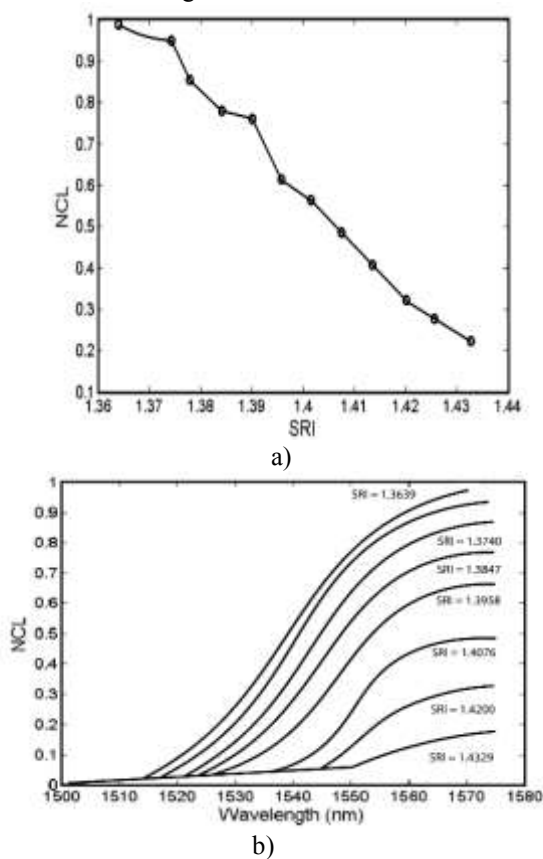


Fig. 11 a,b Change of normalized circuit length along with change of SRI (on the left), change of normalized circuit length along with the wavelength for separate SRI (on the right).

To compute the calibration curve there is selected the wavelength range. In the given case, there was used the range from 1500 to 1555 Nm. Specifying the point on calibration curve (Figure 11) dependences of wavelength cut off on refractive index for each measured spectrum might be presented as follows.

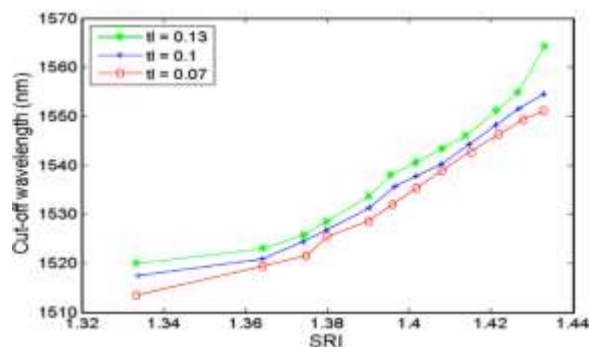


Fig. 12 Dependence of wavelength on external refractive index for three levels.

As can be seen from Figure 12, the position depends on the intersection point of the cycle length curve and the selected threshold level. This level should be selected individually for each type of grid.

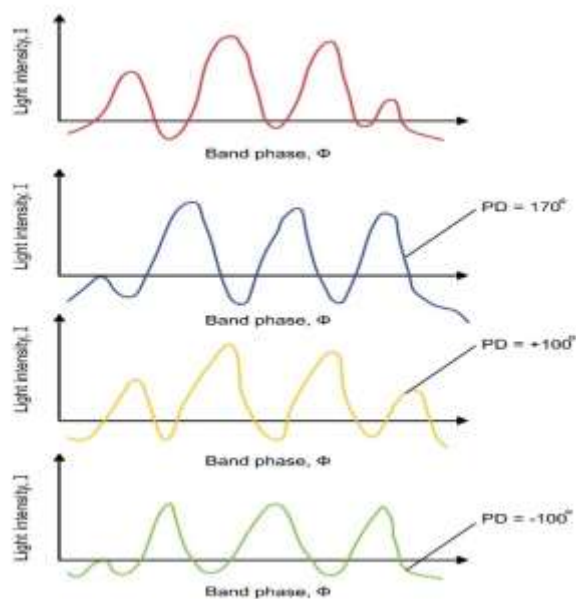


Fig. 13 Dependences of light intensity distribution along band's normal: F-band phase, I-band intensity, and PD-phases difference of two sequential band images.

Figure 13 shows line boundary. Presents phases sequential pictures.

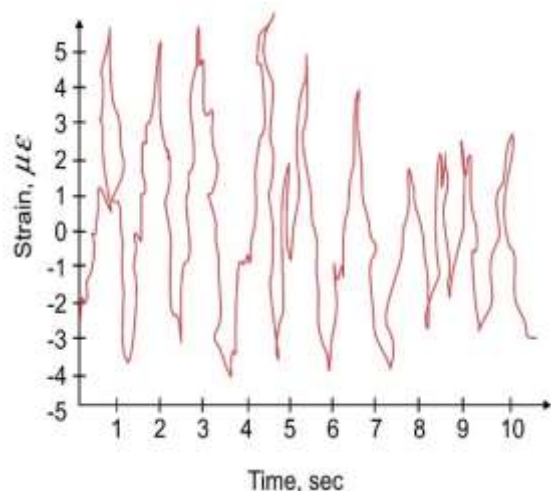


Fig. 14 Deformation dependence on time

Experimental deformation-time, shown in Figure 14 occurs upon free low-frequency vibration with amplitude attenuation. There exists approximately the same sampling interval when a signal can't be received. Figure 15 shows, that the deformation amplitude gradually decreases due to the damping effect.

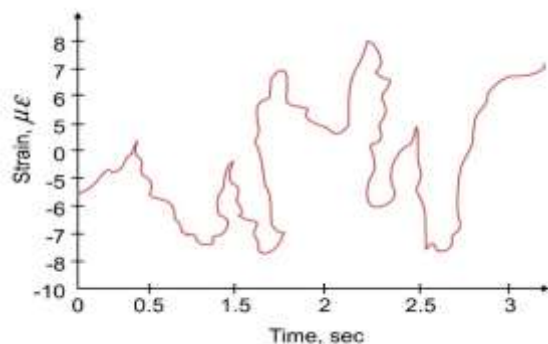


Fig. 15 Deformation dependence on temporary random vibration response upon wind load on fiber-optic sensor with tilted Bragg grating

Figure 15 shows the dependence of deformation on the time response of random vibration under wind load on a fiber-optic sensor with an inclined Bragg grating. The deformation for the sensor response to wind vibration has a nonlinear structure. After 0.5-1.5 seconds, the response decreases, since this sensor is very sensitive to various influences, especially to electromagnetic interactions.

#### IV. DISCUSSION

Measurements of a photonic fiber-optic pressure sensor with an inclined Bragg grating were carried out in water with a salt solution. The grating used had an inclination angle of  $\theta = 8$  and was maintained using the phase mask method. The spectrum measurements were carried out with a determination of 0.01 Nm. The researchers did everything possible to preserve the lattice to avoid additional bends. The grating spectrum is mainly influenced by the angle of inclination, the length of the grating, and the depth of its distribution along the

length of the grating (anodizing). The range is selected to calculate the calibration curve. In this case, the range from 1500 to 1555 Nm. m was used. The work herein has considered the technique for measuring low-frequency vibration of the system with tilted Bragg grating. In the future, a photonic fiber-optic pressure sensor will be made and studied in full-scale form. Critical discussion of the results of this study, we proposed a new sensitive device for high-precision and sensitive pressure detection. To implement the pressure sensor device, the refractive indices of materials were taken into account. The refractive index, which is sensitive to deformation in the developed sensor, is the main factor in achieving this goal. The results obtained indicate significant changes in the refractive indices of these materials under applied pressure. Consequently, the sensitivity of the multimode mode, which is formed inside the photonic band gap, is very high to pressure changes. The study revealed a relatively high sensitivity of the proposed sensor, which can reach 15.23 THz/HPa or 123.43 nm/HPa.

#### V. CONCLUSIONS

The article herein presents the development of optical elements of signal and interrogation demodulation systems from photonic pressure sensors. There was developed a new model of the photonic pressure sensor. An important feature of the given model is a special metal diaphragm, which being deformed rejects a cantilever, as a result of which the gratings are recorded on the same multimode fiber. Also, there is photonic-crystal fiber, which induces multimode fibers. In the work herein there was used the loop method, which makes computations of length for a spectrum, inceptive from the side of shorter waves. During the research, the grating transmittance spectrum was positioned in the air. The grating spectrum, according to the research, is mainly influenced by a tilt angle, grating length, refractive index modulation depth, and its distribution along the grating length (apodization). As well, spectra of photonic fiber-optic pressure sensor with tilted Bragg grating emerged into water with saline solution for several hours, where cladding modes disappear from the side of shorter waves while SRI increases. The value at the intersection point of the contour length curve and the selected threshold level was calculated. In the research herein it was found, that, on the whole, coherency constitutes 4%. It means, that the method is reliable for measuring random vibration. Also, there is obtained image frequency, which is 25 Hz, i.e., 25 image frames per second. It proves that band movement frequency shall be less, than 10 Hz.

#### ACKNOWLEDGMENT

This work is supported by grant from the Ministry of Education and Science of the Republic of Kazakhstan within the framework of the Project № AP09259547 «Development of a system of distributed fiber-optic sensors based on fiber Bragg gratings for monitoring the state of building structures», Institute Information and Computational Technologies CS MES RK. Experimental researches have been carried out in the laboratories of optoelectronics at the Electric engineering

and computer sciences faculty of Lublin Technical University.

### References

- [1] M.Yin, B.Gu, Q.An, C.Yang, Y.Guan, K.Yong, "Recent development of fiber-optic chemical sensors and biosensors: Mechanisms, materials, micro/nano-fabrications and applications. *Coordination Chemistry Reviews*", vol.2, no.376, pp.348-392,2018.
- [2] X.Chen, J.Xu, X.Zhang, T.Guo, B.Guan, "Wide range refractive index measurement using a multi-angle tilted fiber Bragg grating. *IEEE Photonics Technology Letters*", vol.29, no.9, 2017.
- [3] A.Ioannou, A.Theodosiou, C.Caucheteur, K. Kalli "Direct writing of plane-by-plane tilted fiber Bragg gratings using a femtosecond laser. *Optics letters*", vol.42, no.24, pp.5198-5201, 2017.
- [4] P.Kisala, D.Harasim, J.Mroczka, "Temperature-insensitive simultaneous rotation and displacement (bending) sensor based on tilted fiber Bragg grating. *Optics express*", vol.2, no.26, pp.29922-29929, 2016.
- [5] S.Cięszczyk, D.Harasim, P.Kisala, "Novel twist measurement method based on TFBG and fully optical ratiometric interrogation. *Sensors and Actuators A: Physical*", vol.272, pp.8-22, 2018.
- [6] D.Harasim, "The Influence of Fibre Bending on Polarization-Dependent Twist Sensor Based on Tilted Bragg Grating. *Metrology and Measurement Systems*", vol. 24, no.3, pp. 577-584, 2017.
- [7] C.Chan, C.Chen, A.Jafari, A.Laronche, A., D.Thomson, J. Albert "Optical fiber refractometer using narrowband cladding-mode resonance shifts. *Applied optics*", vol.46, no.7, pp.1142-1149, 2007.
- [8] C.Zhao, X.Yang, M.Demokan, W.Jin, "Simultaneous temperature and refractive index measurements using a 3 slanted multimode fiber Bragg grating. *Journal of lightwave technology*", vol.24, no.2, pp. 879-883, 2006.
- [9] A.Wong, M.Giovinazzo, H.Tam, C.Lu, G. Peng "Simultaneous two-parameter sensing using a single tilted Moiré fiber Bragg grating with discrete wavelet transform technique. *IEEE Photonics Technology Letters*", vol.22, no.21, pp.1574-1576, 2010.
- [10] G.Laffont, P.Ferdinand "Tilted short-period fibre-Bragg-grating-induced coupling to cladding modes for accurate refractometry. *Measurement Science and Technology*", vol.12, no.7, pp.765-770, 2001.
- [11] C.Caucheteur, P.Mégret "Demodulation technique for weakly tilted fiber Bragg grating refractometer. *IEEE Photonics Technology Letters*", vol.17, no.12, pp.2703-2705, 2005.
- [12] L. B.Melo, J. M.M. Rodrigues, A. S. F.Farinha, C. A.Marques, L.Bilro, N.Alberto, R. N.Nogueira "Concentration sensor based on a tilted fiber Bragg grating for anions monitoring. *Optical Fiber Technology*", vol.20, no.4, pp.422-427, 2014.
- [13] Z.Liu, C.Shen, Y.Xiao, J.Gong, J.Wang, T.Lang, C.Zhao, C.Huang, Y.Jin, X.Dong, Y.Zhang, Z.Jing, W.Peng, Y.Semenova "Liquid surface tension and refractive index sensor based on a tilted fiber Bragg grating. *J. Opt. Soc. Am.*", vol.35, pp.1282-1287, 2018.
- [14] W.Zhou, D. J.Mandia, S. T.Barry, J.Albert "Absolute near-infrared refractometry with a calibrated tilted fiber Bragg grating. *Optics letters*", vol.40, no.8, pp. 1713-1716, 2015.
- [15] T.Osuch, T.Jurek, K.Markowski, K.Jedrzejewski "Simultaneous measurement of liquid level and temperature using tilted fiber Bragg grating. *IEEE Sensors Journal*", vol.16, no.5, pp.1205-1209, 2016.
- [16] Y.García, J.Corres, J.Goicoechea, "Vibration Detection Using Optical Fiber Sensors. *Journal of Sensors*", pp.1-12, 2010
- [17] T.Giallorenzi, J.Bucaro, A.Dandridge "Optical fiber sensor technology. *IEEE Journal of Quantum Electronics*", vol.18, no.4, pp. 626-665, 1982.
- [18] J. Vento, F.Lopez-Hernandez, A.Santamaria-Rperez; R.Perez-Jimenez, J. Rabadan "Infrared wireless DSSS system for indoor data communication links. *Optical Wireless Communications II 1999*", vol.3850, pp.92-99, 1999.
- [19] R.Hongbin, J.Jinlei, J.Zhishe, Z.Dengyu, "Application of Spread Spectrum Technology to Measurement, Air Force Institute of Missile, Shaanxi, China", 1997.
- [20] G.Perrone, A.Vallan "A low-cost optical sensor for noncontact vibration measurements. *IEEE Transactions on Instrumentation and Measurement*" vol.58, no.5, pp.1650-1656, 2009.
- [21] B.Culshaw "Optical Fibre Sensing and Signal Processing; P. Pergrinus, London, UK", 1984.
- [22] N.Aydin, T.Arslan, T.Cumming "A direct-sequence spread-spectrum communication system for integrated sensor microsystems. *IEEE Transactions on Information Technology in Biomedicine*", vol.9, no.1, pp.4-12, 2005.
- [23] G.Pitt, P.Extance, R.Neat "Optical-fibre sensors. *IETE Technical Review*", vol.9, no.8, pp.379-417, 1986.
- [24] U.Gunasilan "Operative factors contributing to the selection of fiber-optic techniques for remote measurement of strain/stress. *In Proceedings of the IEEE 9th International Conference on Computer and Information Technology*, Xiamen, China, 11-14 Oct.", 2009.
- [25] J.Hecht, "Understanding Fiber Optics; Pearson Prentice Hall, NJ, USA", 2006.
- [26] S. Ione, N.Limanova "Fiber-optic sensor. Patent RU", no.2267085, 27.12.2005.
- [27] T.Gangopadhyay, S.Chakravorti, S.Chatterjee, K.Bhattacharya "Multiple fringe and nonsinusoidal signals obtained from a fiber-optic vibration sensor using an extrinsic Fabry-Perot interferometer. *Measurement Science and Technology*", ni.16, pp.1075-1082, 2005.
- [28] X.Zhang, X.Liu, F.Zhang, Zh.Sun, L.Min, Sh.Li "Reliable high sensitivity FBG geophone for low frequency seismic acquisition. *Measurement*", no.129, pp.62-67, 2018.
- [29] X.Zhang, Q.Rong, H.Sun, Sh.Yang, L.Yuan, M.Hu "Low-frequency fiber Bragg grating accelerometer based on a double-semicircle cantilever. *Optical Fiber Technology*", no.20, pp.190-193, 2014.
- [30] Y.Zhang, X.Qiao, Q.Liu, D.Yu, H.Gao, M.Shao "Study on a fiber Bragg grating accelerometer based on compliant cylinder. *Optical Fiber Technology*", no.26, pp.229-233, 2015.
- [31] Y.Weng, X.Qiao, T.Guo, M.Hu, Zh.Feng, R.Wang "A Robust and compact Fiber Bragg Grating vibration sensor for seismic measurement. *IEEE Sensors journal*", vol.12, no.4, pp.800-804, 2011.
- [32] X.Weng, Y.Guo, L.Xiong, H.Wu "High Frequency Optical Fiber Bragg Grating Accelerometer. *IEEE Sensors journal*", vol.18, no.12, pp. 4954-4960, 2018.
- [33] A.Kalizhanova, M.Kunelbayev, A.Kozbakova, Zh.Aitkulov, Zh.Orazbekov "Computation of temperature, deformation and pressure in engineering and building structures using fiber Bragg sensor with tilted grating in Kazakhstan. *Materials Today: Proceedings*", vol.50, no.5, pp.133-1340, 2022.

**Contribution of individual authors to the creation of a scientific article (ghostwriting policy)**

Aliya Kalizhanova conducted an organizational moment for a demodulation system and vibration signals for a photonic fiber-optic pressure sensor

Murat Kunelbayev, Ainur Kozbakova organized and performed the experiments described in section 3

Waldemar Wojcik, Baydaulet Urmashiev, Assiyat Akhustova has organized and executed the experiments of Section 3.

**Sources of funding for research presented in a scientific article or scientific article itself**

This work is supported by grant from the Ministry of Education and Science of the Republic of Kazakhstan within the framework of the Project № AP09259547 «Development of a system of distributed fiber-optic sensors based on fiber Bragg gratings for monitoring the state of building structures», Institute Information and Computational Technologies CS MES RK. Experimental researches have been carried out in the laboratories of optoelectronics at the Electric engineering and computer sciences faculty of Lublin Technical University.

**Conflict of Interest**

The authors have no conflict of interest to declare that is relevant to the content of this article.

**Creative Commons Attribution License 4.0 (Attribution 4.0 International, CC BY 4.0)**

This article is published under the terms of the Creative Commons Attribution License 4.0

[https://creativecommons.org/licenses/by/4.0/deed.en\\_US](https://creativecommons.org/licenses/by/4.0/deed.en_US)